Effect of autaptic delay signal on spike-timing precision of single neuron

Xuan Ma(马璇)[1], Yaya Zhao(赵鸭鸭)[1], Yafeng Wang(王亚峰)[2], Yueling Chen(陈月玲)[3], and Hengtong Wang(王恒通)[1,†]

[1] *School of Physics and Information Technology, Shaanxi Normal University, Xi'an* 710119, *China*
[2] *School of Physics and Information Technology, Baoji University, Baoji* 710062, *China*
[3] *College of Information Engineering, Gansu University of Chinese Medicine, Lanzhou* 730000, *China*

(Received 19 March 2022; revised manuscript received 11 May 2022; accepted manuscript online 29 May 2022)

Experimental and theoretical studies have reported that the precise firing of neurons is crucial for sensory representation. Autapse serves as a special synapse connecting neuron and itself, which has also been found to improve the accuracy of neuronal response. In current work, the effect of autaptic delay signal on the spike-timing precision is investigated on a single autaptic Hodgkin–Huxley neuron in the present of noise. The simulation results show that both excitatory and inhibitory autaptic signals can effectively adjust the precise spike time of neurons with noise by choosing the appropriate coupling strength g and time delay of autaptic signal τ. The g–τ parameter space is divided into two regions: one is the region where the spike-timing precision is effectively regulated; the other is the region where the neuronal firing is almost not regulated. For the excitatory and inhibitory autapse, the range of parameters causing the accuracy of neuronal firing is different. Moreover, it is also found that the mechanisms of the spike-timing precision regulation are different for the two kinds of autaptic signals.

Keywords: autapse, time delay, spike-timing precision

PACS: 87.19.lg, 87.19.ll **DOI:** 10.1088/1674-1056/ac7451

1. Introduction

The accurate sensory representation makes living creatures avoid danger, get food and survive in cruel nature.[1,2] Both experimental and theoretical studies reveal that precise firing of neurons is crucial to correcting the sensory representation.[3–5] Sensory neurons transmit different external sensory stimuli, such as sound, taste, and touch, into firing patterns with different temporal characteristics.[6] Sensory information is processed in the neocortex and eventually integrated into various behavioral and cognitive function.[7] In these processes, cortical neurons represent information by generating discrete action potential (AP) sequences with precise time.[6] The spike-timing precision of spikes in visual neurons carries a wealth of time-varying visual stimulus information,[8,9] and auditory neurons in the auditory brain stem encode information according to the time of a single peak.[10–12] The precise timed action potentials (APs) are believed as one way of the temporal coding, and have been found in many experiments.[13,14]

Understanding neuronal coding is one of the most important fundamental problems in neuroscience and computational neuroscience. The brain's ability to accurately represent sensory and other information through neurons means it can accurately characterize and respond to information.[16,17,46] Thus, many research works focus on characterizing the relationship between the stimulus and the individual or ensemble neuronal responses.[18,19] In vitro, identical step current injection produces very jittery firing in pyramidal neurons in neocortical slices, but the spike-timing precision is significantly improved when the injected current contains synaptic-like noise.[5] The spike time can be regulated by synaptic plasticity, which has been observed at the cerebellum.[20,21] It is also reported that many factors, in current researches, affect the accurate response of neurons to signals, such as the noise of ion channel switch[2] and special ion current.[23,24]

It is more interesting that a quite precise firing in neocortical fast-spiking interneurons is due to the autaptic connection,[25,27–29] which is the special synapse that connects the neuron to itself and constitutes the smallest network in the nervous system.[30,31] The experimental results also reveal that autapse promotes the accuracy of neuronal firing and regulates the activities of the nervous system.[29,32–36] Nevertheless, the function of autapses and their contribution to the accuracy of neuronal firing are still unclear. Thus, understanding the effect of autaptic activities on accurate neuronal responses is still critical work.

In the present work, we intend to reveal the dynamical properties of the autaptic regulation on the accurate neuronal response. Moreover, due to the limited propagation speed of the action potential on the axon and time-lapse of information transmission in the synaptic process and signal reception in the dendritic process, the signal received by postsynaptic

†Corresponding author. E-mail: wanghengtong@snnu.edu.cn
© 2023 Chinese Physical Society and IOP Publishing Ltd

neuron has a long time delay compared with the time generation of action potential on the presynaptic neuron. It has been reported that such time delay is a fundamental part of almost all biological phenomena in nervous systems and can improve the function of the neural network (synchronization and stability).[37–39] Thus, the time delay of the signal is considered in the current work.

The structure of the paper is as follows. In Section 2, we introduce the neuronal and synaptic models and the measurement of spike-timing precision. Section 3 contains the results of spike-timing precision of neuron without or with autapse. Finally, the conclusions and discussions are summarized in Section 4.

2. Model and methods

In the 1950s, Hodgkin and Huxley established a neuronal model (named as HH model) with a fourth-order differential equation based on the experimental data.[40] This model presents the basic characteristics of neuronal ion channels and action potential generation. Since there are full of random influence on the trans-membrane voltage of a single neuron, the white Gaussian noise is introduced to the neuronal model. Thus, the expression of the autaptic HH model is as follows:

$$\begin{aligned} C_{\rm m}\frac{{\rm d}V}{{\rm d}t} &= -g_{\rm Na}m^3h(V-E_{\rm Na})-g_{\rm K}n^4(V-E_{\rm K}) \\ &\quad -g_{\rm L}(V-E_{\rm L})+I_0+I_{\rm aut}+\xi(t), \qquad (1) \\ \frac{{\rm d}x}{{\rm d}t} &= \alpha_x(1-x)-\beta_x x, \quad (x=m,h,n). \qquad (2) \end{aligned}$$

Here, $C_{\rm m}=1$ μF/cm^2 is the membrane capacitance. m, h and n are gating parameters of the Na^+ and K^+ ion channels, and depend on the membrane potential V and time t. $g_{\rm Na}=120$ mS/cm^2, $g_{\rm K}=36$ mS/cm^2 and $g_{\rm L}=0.3$ mS/cm^2 denote the maximum conductances of sodium, potassium and leakage currents, respectively. The reversal potentials corresponding to the three kinds of transmembrane ion currents are set as $E_{\rm Na}=50.0$ mV, $E_{\rm K}=-77.0$ mV and $E_{\rm L}=-54.5$ mV. I_0 is external DC stimulus (a based current) injected in neuron. $\xi(t)$ stands for white Gaussian noise satisfying $\langle\xi(t)\rangle=0$ and $\langle\xi_i(t_1)\xi_j(t_2)\rangle=2D\delta_{i,j}\delta(t_1-t_2)$, with the noise intensity D. α and β determine the rate of ion transfer from outside to inside. The equations of α and β satisfy

$$\begin{aligned} &\alpha_m=0.1\frac{V+40}{1-{\rm e}^{-(V+40)/10}}, \quad \beta_m=4\,{\rm e}^{-(V+65)/18}, \\ &\alpha_h=0.07\,{\rm e}^{-(V+65)/20}, \quad \beta_h=\frac{1}{1+{\rm e}^{-(V+35)/10}}, \\ &\alpha_n=0.01\frac{V+55}{1-{\rm e}^{-0.1(V+55)}}, \quad \beta_n=0.125\,{\rm e}^{-(V+65)/80}. \qquad (3) \end{aligned}$$

Autaptic current $I_{\rm aut}$ is based on the following equations:

$$\begin{aligned} I_{\rm aut}(t) &= G(t-\tau)(V-E_{\rm aut}), \\ G(t) &= g\sigma(t-t_{\rm fire}), \\ \sigma(t) &= \frac{\exp(-t/t_{\rm d})-\exp(-t/t_{\rm r})}{t_{\rm d}-t_{\rm r}}, \qquad (4) \end{aligned}$$

where $G(t-\tau)$ is the autaptic conductance with time delay τ of the presynaptic signal and $E_{\rm aut}$ represents autaptic reversal potential. $E_{\rm aut}=0$ mV represents excitatory autapse and $E_{\rm aut}=-80$ mV represents inhibitory autapse. g is autaptic coupling strength. $t_{\rm fire}$ is time of presynaptic spike. $t_{\rm d}=3.0$ ms and $t_{\rm r}=0.1$ ms represent the decay and rise time, respectively.

Multi-sample statistics of neuronal action potential firing sequences have been borrowed to determine the accuracy of neuronal spike-timing. The spike-timing precision of neuronal response to a stimulus is calculated by the standard deviation of the ordinal spike times across multiple parallel stimulation trials,[29]

$$s_n=\sqrt{\frac{\sum_{i=1}^{N}(t_i^n-\bar{t}^n)^2}{N}}. \qquad (5)$$

Here, t_i^n is the time of the nth action potential in the ith simulation trail, and $\bar{t}^n$ is the average time of the nth number of action potential in N simulations.The result of the standard deviation s_n is named as spike jitter of the neuronal spike time. The smaller the jitter is, the more accurate the neuronal response is.

In order to quantify trail-to-trail change, instantaneous firing rate is usually used as the characteristic quantity of time series. This firing rate is only dependent on the stimulus and the spike sequence before it. The firing rate of the neuron across multiple parallel stimulation trials is given below:[41]

$$P_{\rm firing}(t)=\lim_{\Delta t\to 0}\frac{1}{\Delta t}\frac{n^{\rm spike}(t,t+\Delta t)}{N}. \qquad (6)$$

Here, $n^{\rm spike}(t,t+\Delta t)$ is the number of spikes between t and $t+\Delta t$, and N is the number of trail. The narrower peak width is, the more accurate encoded information is. In current work, the number of trail N is chosen as 4500 and $\Delta t=0.1$ ms.

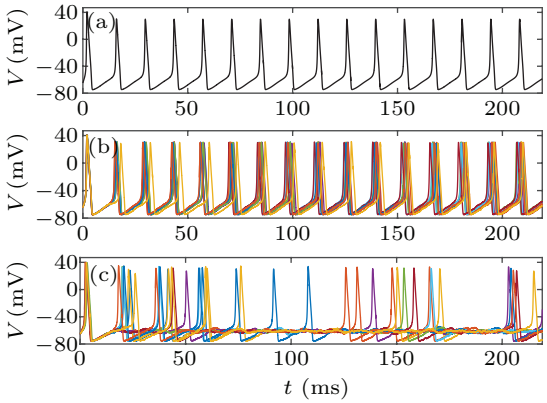


Fig. 1. The membrane potential of the HH neuron is stimulated by different DC in various noise environments. (a) The neuron is stimulated by super-threshold DC without noise. (b) and (c) The neurons are stimulated by either super- or sub-threshold DC with noise $D=0.5$ mA/cm^2. (a) and (b) $I_0=12.0$ mA/cm^2. (c) $I_0=6.0$ mA/cm^2.

3. Results

3.1. Neuron without autapse

Under super-threshold DC stimulus, the HH neuron without autapse exhibits regular spiking. As shown in Fig. 1(a), the regular spiking has been triggered by super-threshold DC stimulus ($I_0 = 12.0$ mA/cm^2). If noise is considered in the simulation, the regular spike time of the HH neuron would be disturbed, seeing in Fig. 1(b). Under the sub-threshold stimulus, the neuron without autapse cannot be triggered as action potentials. But, as the noise is large enough, the neuron without autapse fires action potentials nearly randomly, as shown in Fig. 1(c).

Comparing AP sequences [Figs. 1(b) and 1(c)], the spike jitter is significantly increased over time, for different simulation trails. In order to determine the accuracy of the spike-timing precision more convenient, the first 16 action potentials of the HH neuron are recorded for each trail and the sub-threshold DC stimulus in a noisy environment is chosen in the following study.

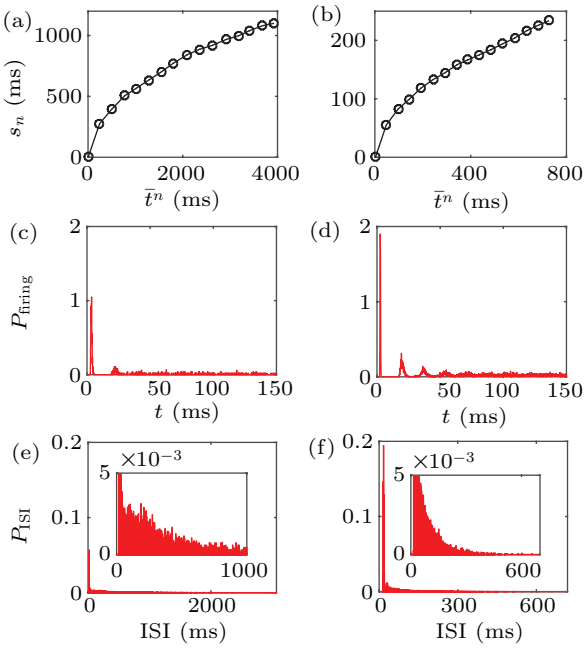


Fig. 2. Spike jitter s_n (a) and (b), firing probability P_{firing} (c) and (d), and statistical histogram of interspike interval P_{ISI} (e) and (f) of HH neuron without autapse stimulated by DC. Left panel: $I_0 = 4.0$ mA/cm^2. Right panel: $I_0 = 6.0$ mA/cm^2. The insets in (e) and (f) are enlarged views of ISI distribution. The intensity of the white noise is chosen as $D = 0.9$ mA/cm^2.

Due to the presence of noise, the spike jitter s_n of the HH neuron without autapse increases over time under sub-threshold DC stimulus [Figs. 2(a) and 2(b)]. For a strong stimulus, the spike jitter is smaller than that of the weak stimulus, and the neuron would spend a shorter time to generating 16 APs. Firing probability P_{firing} of the HH neuron without autapse reveals the trail-to-trail change of spike time [Figs. 2(c) and 2(d)]. With time evolution, there are no more peaks, but a strong stimulus can trigger more peaks in the curve of firing probability than the weak stimulus (three peaks can be found in Fig. 2(d)). That is the result the strong stimulus inhibits randomness of noise. Figures 2(e) and 2(f) show the statistical histogram of interspike interval (ISI). Here, the ISIs are distributed in the range of 0–3000 ms [Fig. 2(e)] and 0–700 ms [Fig. 2(f)]. It is easy to observe that the ISIs distribution in Fig. 2(f) is more concentrated than that in Fig. 2(e). That is to say, ISIs distribution of the neuron stimulated by a stronger DC stimulus is more concentrated. It is revealed that the increase in stimulus intensity can improve spike-timing precision. It is also noted that it would be found that the precision of the spike-timing could be largely regulated by introducing autapse in the following part.

3.2. Neuron with excitatory autapse

In this part, excitatory autapse is introduced to the HH neuron. Figure 3 represents the changes in spike-timing precision with different time delays and coupling strength. Comparing the subfigures in Fig. 3, it is clear that the precision of the spike time has been largely regulated by the excitatory autapse. The curves with different colors and markers represent the evolution of jitter with different time delays for each subfigure. In Fig. 3(a), it can be seen that the spike jitter s_n of excitatory autaptic neuron with time delay $\tau = 3.0$ ms, 7.2 ms and 9.0 ms does not change greatly compared with that of neuron without autapse. As the time delay increases, the spike jitter s_n decreases greatly, and the average time been taken to generate 16 APs also decreases sharply (the lines with time delay $\tau = 10.2$ ms and 12.6 ms). Further increasing the time delay, the spike jitter s_n first increases and subsequently decreases. Moreover, with the stronger coupling strength [Figs. 3(b)–3(d)], the range of the time delay τ to effectively reduce the spike jitter is enlarged. It is noted that the spike jitter s_n could be adjusted to a very low degree by the delayed autaptic signal as the appropriate time delay and coupling strength are selected. More specifically, the autapse with some special time delays can weaken the effect of noise and improve the precision of APs. Moreover, the spike jitter s_n increases in time sequence as a whole. This rule does not depend on time delay and coupling strength, even the jitter is adjusted to a very low value.

To check the impact of time delay on the background behaviors of the spike-timing precision, the autaptic coupling strength is set as a constant ($g = 0.2$ mS/cm^2) in Fig. 4. It is clear that the statistical histogram of ISIs of neuron with excitatory autapse becomes more concentrated, as the time delay increases in Figs. 4(a)–4(c). When the time delay is set as 9.0 ms [Fig. 4(a)], the ISIs are distributed in a very large area (12–1500 ms). As the time delay is increased to 10.2 ms in Fig. 4(b), the amount of large ISIs has been decreased and the ISIs become more concentrated. At $\tau = 12.6$ ms in Fig. 4(c),

the ISIs are almost concentrated near 16 ms. The probabilities of spikes occurring times are plotted trail-to-trail in Figs. 4(d)–4(f). Here, we can see in each subfigure that peaks of the firing probability P_{firing} are gradually lower and broader, which means that the spike-timing precision is becoming poor as the time evolves. However, as the time delay increases from 9.0 ms to 12.6 ms, the peaks of P_{firing} are enhanced. It is also revealed that the spike-timing precision is improved by the autapse. Raster plots of spike time given in Figs. 4(g)–4(i) exhibit the spike time of the neuron for 500 different stimulus trials. As shown in Fig. 4(g), it is clear that the neuron fires APs nearly randomly as the time delay is 9.0 ms similar to that of neuron without autapse in Fig. 1(c). As the time delay increases, the spike time plots move to the left, and the spikes of the neuron with a time delay 12.6 ms are nearly the same time for different simulation trails. Those background information reveals that the addition of autapse improves the regularity of APs and the ISIs of the autaptic neuron are almost concentrated at a certain value by choosing the appropriate time delay.

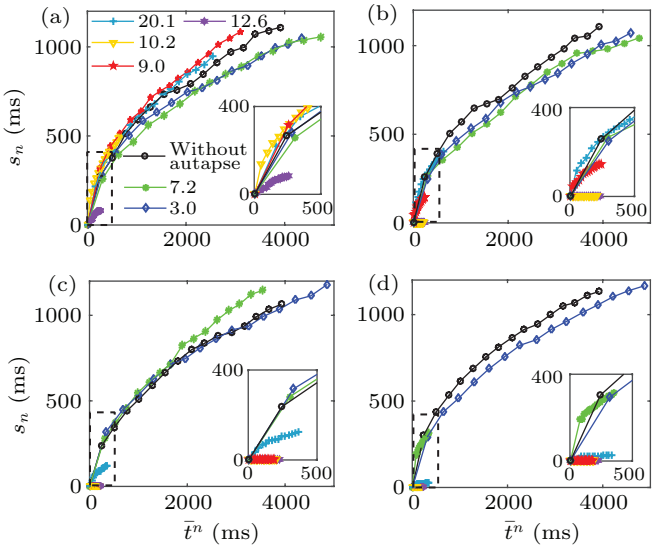


Fig. 3. Spike jitter s_n of neuron with and without excitatory autapse for different time delay τ and coupling strength g. (a)–(d) s_n of the HH neuron without autapse are presented by black lines and s_n of the neuron with autapse are presented by different color lines. The coupling strength is set as (a) $g = 0.2$ mS/cm^2, (b) $g = 0.4$ mS/cm^2, (c) $g = 0.6$ mS/cm^2 and (d) $g = 0.8$ mS/cm^2. The insets in (a)–(d) are enlarged views of spike jitter. The based DC stimulus is chosen as $I_0 = 4.0$ μA/cm^2.

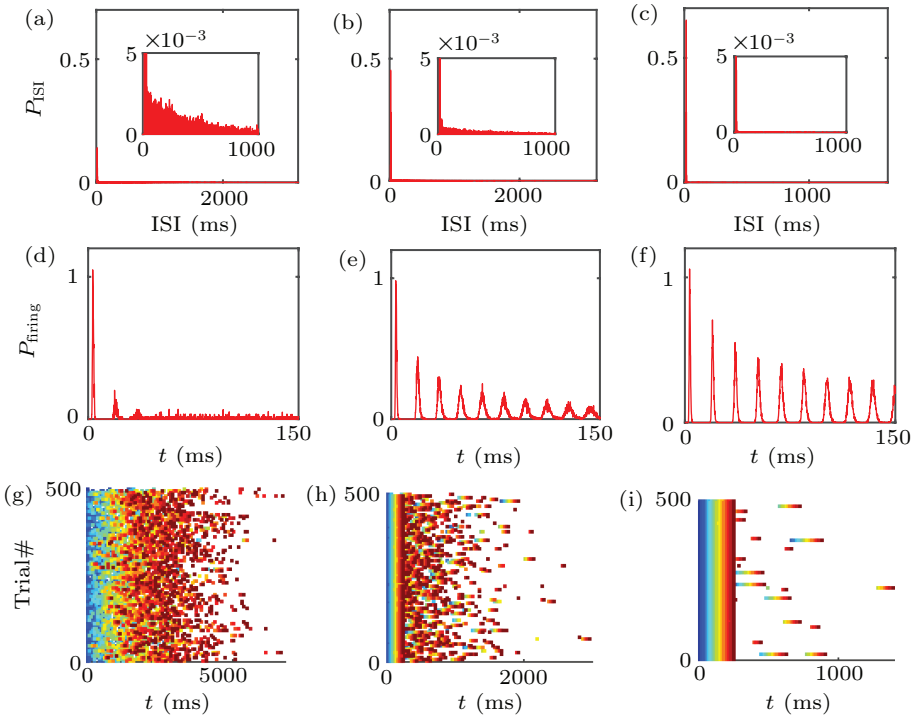


Fig. 4. Statistical histogram of the interspike interval P_{ISI} (a)–(c), firing probability in 150 ms P_{firing} (d)–(f) and raster plot of spike time (g)–(i) of neuron with excitatory autapse stimulated by DC. The same color in the raster plots means the same order number of the corresponding AP in different simulation trails. Left panel: $\tau = 9.0$ ms. Middle panel: $\tau = 10.2$ ms. Right panel: $\tau = 12.6$ ms. The coupling strength is set as $g = 0.2$ mS/cm^2. The based DC stimulus is chosen as $I_0 = 4.0$ μA/cm^2.

Figure 5 shows the ISI probability, firing probability, and raster plot of spike time for different coupling strength (from the left to right panel). With the increase of the coupling strength, the distribution of ISIs becomes more and more concentrated. As the coupling strength is lower [e.g., Fig. 5(b), $g = 0.4$ mS/cm^2], the ISIs are near randomly distributed in a large area. Increasing the coupling strength [e.g., Fig. 5(b), $g = 0.6$ mS/cm^2], the ISIs is compressed and distributed in the range of 12–13 ms. When the coupling strength is strong enough [e.g., Fig. 5(c), $g = 0.8$ mS/cm^2], the ISIs of all the simulation trails are all concentrated at 12 ms. It can be also observed that the number of the peaks of the firing probability increases and the peaks become higher and narrower with the increase of coupling strength [Figs. 5(d)–5(f)]. Moreover, the

raster plot of spike time also reveals that the action potential sequence is almost a regular sequence, as the coupling strength is high enough [Figs. 5(g)–5(i)].

In Fig. 6(a), the spike jitter of the 16th spike s_{16} is characterized by the function of coupling strength and time delay. There are obviously two regions in the g–τ plane: one is the region where the autaptic signal can effectively regulate the spike-timing precision (s_{16} is regulated below 200, seeing the blue area); the other is the region where the neuronal firing is almost not been regulated (the spike jitter is not below 1000 seeing the orange area). For the autaptic signal with a short time delay or weak coupling strength, it is clear that the spike jitter is very large. However, the spike jitter is very low for the autaptic signal with a long time delay and strong coupling strength. Remarkably, the jitter evolution of the 16th spike in Fig. 6(a) is similar to that of the other order spikes. It is also noted that the reason for two different regulatory regions presented in Fig. 6(a), is that the autaptic signals have different effects on neuronal firing in these two areas. The autaptic signals with the parameters in the orange area can not trigger the HH neuron but can trigger the neuron in the blue area.

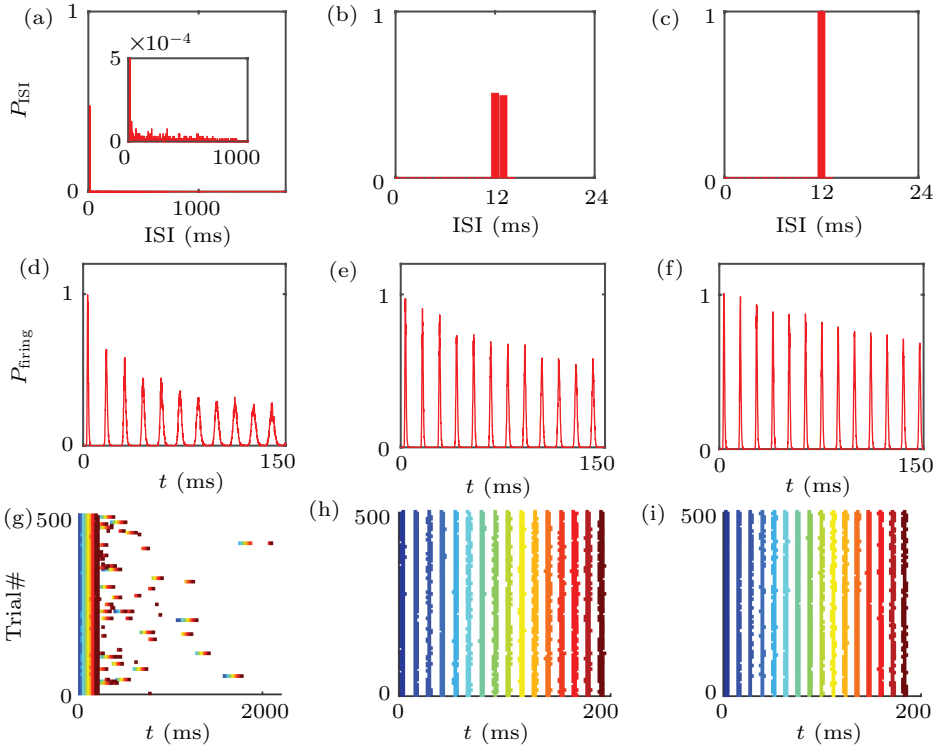


Fig. 5. Statistical histogram of the interspikie interval $P_{\rm ISI}$ (a)–(c), firing probability in 150 ms $P_{\rm firing}$ (d)–(f) and raster plot of spike time (g)–(i) of the neuron stimulated by DC with different excitatory autaptic coupling strength. The same color in the raster plots means the same order number of the corresponding AP in the different simulation trails. Left panel: $g = 0.4$ mS/cm^2. Middle panel: $g = 0.6$ mS/cm^2. Right panel: $g = 0.8$ mS/cm^2. The time delay is set as $\tau = 9.0$ ms. The based DC stimulus is chosen as $I_0 = 4.0$ μA/cm^2.

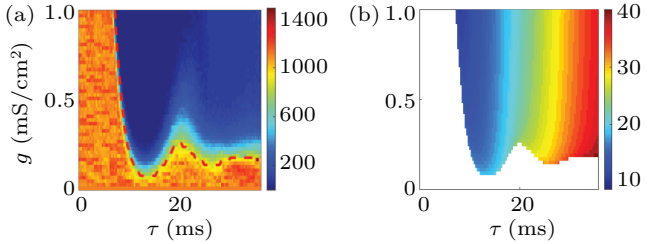


Fig. 6. (a) Spike jitter of the 16th spike s_{16} as a function of the coupling strength and time delay. The color tends to be cold and the higher spike-timing precision it is. (b) State of excitatory autaptic neuron stimulated by a single super-threshold pulse in the noise free environment. The autaptic signal with the parameters (time delay and coupling strength) in the white area cannot produce continuous APs, but that with the parameters in the colored area can. The color represents the firing period. The red dash line in (a) is the boundary of the color area in (b). The based DC stimulus is chosen as $I_0 = 4.0$ μA/cm^2.

In order to explain the induction mechanism of the above phenomena, Fig. 6(b) illustrates the state of excitatory autaptic neuron stimulated by a single super-threshold pulse as the function of autaptic coupling strength g and the time delay τ. It is clear that the g–τ plane is divided into two regions: the colored area indicates that the neuron with the autaptic parameters in the colored area can be triggered continuous neuronal oscillations, but the blank area means the neuron with the parameters in the area can not be triggered. Comparing Figs. 6(a) and 6(b), it could be found that the region divisions on the g–τ plane are consistent with each other. This reveals that the regulation of autapse on the firing accuracy of a single neuron under a noise background depends on whether the autaptic signal received by the neuron can induce sustained super-threshold oscillation. When the coupling strength is small, the autaptic signal received by the neuron can not induce the neuronal firing in the noise background, so the firing of the neu-

ron is almost random and the spike-timing precision is poor. As the coupling strength is increased, the autaptic pulse signal superimposed with background noise gradually stimulates the neuron to produce APs. For the autaptic signal with large coupling strength but short time delay, the signal can not produce effective continuous oscillation, although the signal can make the neuron to release a single AP. That is because when the latter pulse signal arrives, the neuron is still in the refractory period and the pulse can not induce an action potential. With the increase in time delay, the arrival time of the autaptic pulse leaves the refractory period of the neuron, and the autaptic pulse could induce the neuron firing. Therefore, the jitter of the neuronal spiking trains is reduced and the spike-timing precision is improved. As the coupling strength and the time delay are both large enough, the autaptic signal could regulate the firing of the neuron. Thus, there is good accuracy area [the blue region in Fig. 6(a)].

3.3. Neuron with inhibitory autapse

In this section, we intend to discuss the effect of inhibitory autapse on the spike-timing precision. Due to the characteristic of inhibitory autapse, small sub-threshold stimulus and noise could not cause the activity of the inhibitory autaptic neuron, we adopt the based DC stimulus (I_0 = 6.0 mA/cm^2) slightly larger than that of the excitatory autaptic neuron. Figure 7 shows the spike jitter s_n of the neuron with and without inhibitory autapse for different time delays and coupling strengths.

Similar to the results of the excitatory autaptic neuron, the spike-timing precision of the neuron is changed by adding inhibitory autapse. When the coupling strength is weak [e.g., Fig. 7(a), $g = 0.2$ mS/cm^2], the spike jitters s_n of the neuron with inhibitory autapse (for different time delays) are similar to that without autapse. The curves of spike jitter s_n vary slightly with the time delay. However, when the time delay is chosen as 13.2 ms, the curve is different from that of other time delays and indicates the enlarged average time taken for the neuron to complete the 16 APs and the worst spike-timing precision. When the coupling strength is increased to $g = 0.4$ mS/cm^2 [Fig. 7(b)], the curve of $\tau = 13.2$ ms is still similar to that of $g = 0.2$ mS/cm^2. For other time delays shown in the subfigure, the curves are still almost clustered together. However, the jitters of the curves are lower than that without autapse. With the continuous increase of the coupling strength [e.g., Fig. 7(c), $g = 0.6$ mS/cm^2], the spike jitter s_n curves for the different time delays τ begin to separate and shrink significantly. It means that the average time taken for the neuron to complete the 16 APs is shortened and the spike-timing precision is improved. When coupling strength is increased to $g = 0.8$ mS/cm^2, for all the time delays shown in Fig. 7(d), the jitters s_n are smaller than that without autapse. It is also interesting that the spike jitter s_n of time delay $\tau = 13.2$ ms is still higher than that of other time delays. It is clear that the regulation of inhibitory autaptic current on spike-timing precision is dependent on the coupling strength and time delay. Moreover, it is also noted that the stronger the coupling strength is, the stronger the regulation effect on the spike-timing precision is.

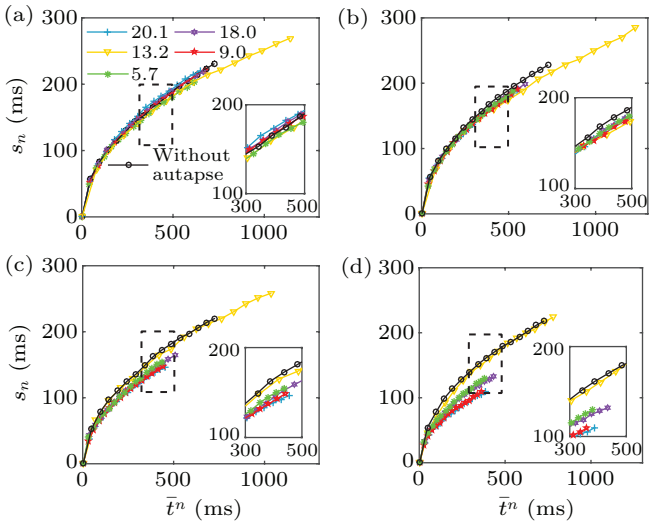


Fig. 7. Spike jitter s_n of neuron with and without inhibitory autapse for different time delay τ and coupling strength g. (a)–(d) s_n of HH neuron without autapse are presented by black lines and s_n of the neuron with inhibitory autapse are presented by different color lines. The coupling strength is set as (a) $g = 0.2$ mS/cm^2, (b) $g = 0.4$ mS/cm^2, (c) $g = 0.6$ mS/cm^2 and (d) $g = 0.8$ mS/cm^2. The insets in (a)–(d) are enlarged views of spike jitter.

Figure 8(a) gives the 16th jitter s_{16} of the neuron with inhibitory autapse in g–τ plane. Similar to the results of excitatory autaptic neuron, there are two regions in the g–τ plane: one is the region in which the autaptic signal can effectively regulate the spike-timing precision (e.g., the spike jitter s_{16} is regulated below 100, see the blue area), and in another region the neuronal firing is almost not been regulated (e.g., the spike jitter s_{16} is above 200, see the orange area). There is also an obvious transitional area between the two regions. Unlike the results of the excitatory autaptic neuron, to obtain better spike-timing precision, a much greater coupling strength is needed for inhibitory autapse. It is interesting that the inhibitory autapse does not improve the spike-timing precision and makes the spikes of the neuron more inaccurate in the range of time delay $\tau = 10$–15 ms and coupling strength g below 1 mS/cm^2. Usually, inhibitory autapse is believed to inhibit the excitation of postsynaptic neurons and make the neuron less likely to generate an action potential. Thus, it is very intriguing to explore how inhibitory autapse regulates neuronal firing accuracy. In Fig. 8(b), the firing behavior of inhibitory autaptic neuron stimulated by a single super-threshold pulse is plotted as the function of autaptic coupling strength g and the time delay τ. The colored area indicates that the neuron with the autaptic parameters in the colored area can be are excited to produce sustained neuronal oscillations (the different colors

indicate different firing periods), but the blank area means the neuron can not be triggered. It is clear that the inhibitory autapse can induce the neuron to fire continuously in the appropriate range of autaptic coupling strength and time delay. The sustained AP firing induced by inhibitory autapse is the famous post-inhibitory rebound (PIR) spikes.[42] As the autaptic coupling strength is weak, the inhibitory autaptic current can not induce the PIR spike and the neuron is only stimulated by the based DC stimulus and noise. Thus, the spike time of the neuron is inaccurate and the jitter s_{16} is high [Fig. 8(a)]. With the increase of the coupling strength, the inhibitory autaptic current can induce the PIR spikes and regulate the neuronal firing. The firing spike time of the neuron is regulated and is getting a little accurate [see the transitional area in Fig. 8(a)]. Further increasing the coupling strength, the effect of the PIR is enhanced and the firing of the inhibitory autaptic neuron is also enhanced. With the change of time delay, the effect of PIR changes, and then the accuracy of neuronal firing changes.

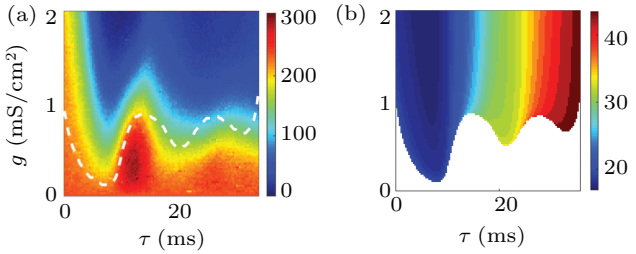


Fig. 8. (a) Spike jitter of the 16th spike s_{16} as a function of the coupling strength and time delay. The color tends to be cold and the higher the spike-timing precision it is. (b) State of inhibitory autaptic neuron stimulated by a single super-threshold pulse in the noise-free environment. The autaptic signal with the parameters (time delay and coupling strength) in the white area cannot produce continuous APs, but that with the parameters in the colored area can. The color represents the firing period. The white dash line in (a) is the boundary of the color area in (b).

4. Discussion and conclusion

Many experiments have revealed that the precisely timed action potential plays an important role in information coding for neurons in the nervous system.[3–6,9,43] It is also reported that a quite precise firing in neocortical fast-spiking interneurons is due to the autaptic connection.[25–29] However, the background mechanism of autapses to the precise neuronal firing is still unclear. In the current work, the model of a single autaptic HH neuron with Gaussian white noise has been constructed to study the effect of the autaptic delay signal on the spike-timing precision. Due to the presence of noise, the spike times of a single neuron stimulated by the same DC-based current are different in the different simulation runs. The firing time of the neuron in different simulation runs becomes more randomly with the increase of the order of the response action potential. In order to describe these phenomena quantitatively, the standard deviation of the ordinal spike times s_n and the firing probability of the neuron $P_{\text{firing}}(t)$ across multiple parallel stimulation trails are introduced in the current work.

When the excitatory autapse is introduced to the HH neuron, the effect of the autaptic signal on the spike-timing precision is dependent on the time delay τ and coupling strength g. For the short time delay, the spike jitter s_n of the excitatory autaptic neuron is similar to that of the neuron without autapse. Increasing the time delay, the spike jitter begins to increase and then decreases. While the coupling strength is increased, the spike jitter s_n would decrease, and the range of the time delay τ to effectively reduce the spike jitter is enlarged. There are two regions in the g–τ parameter space: one is the region where the spike-timing precision is effectively improved; another is the region where the neuronal firing is almost not regulated. The regulation of excitatory autapse on the firing accuracy is found to depend on whether the autaptic signal received by the neuron can induce sustained action potential response. For the small coupling strength, the autaptic signal received by the neuron can not induce the neuronal firing in the noise background, so the firing of the neuron is almost random and the spike-timing precision is poor. As the coupling strength is increased, the autaptic pulse signal superimposed with background noise gradually stimulates the neuron to produce an action potential. For an autaptic signal with large coupling strength but short time delay, although the signal can make a neuron release action potential, it can not produce effective continuous oscillation. That is because when the latter pulse signal arrives, the neuron is still in the refractory period and the pulse can not induce an action potential. With the increase in time delay, the arrival time of autaptic pulse leaves the refractory period of the neuron, and the autaptic pulse could induce the neuron to fire. Therefore, the jitter of the neuronal spiking trains is reduced and the spike-timing precision is improved. As the coupling strength and the time delay are both larger enough, the autaptic signal could regulate the firing of the neuron.

Similar to the results of the excitatory autaptic neuron, the spike-timing precision of the inhibitory autaptic neuron also depends on the time delay τ and coupling strength g. In the g–τ plane, there are also the region where the autaptic signal can effectively regulate the spike-timing precision and the region where the neuronal firing is almost not been regulated. Unlike the excitatory autapse, a greater coupling strength is needed for inhibitory autapse to obtain better spike-timing precision. Moreover, it could be more interesting that the inhibitory autaptic signal can trigger the neuron firing action potential and improve the spike-timing precision, although the inhibitory input is believed typically to lower neuronal excitability. The inhibitory autaptic signal with weak coupling strength and short time delay cannot induce the neuron to fire continuously. However, with the appropriate coupling strength and time delay, the inhibitory autaptic signal can induce the continuous action potentials, due to the famous mechanism

of post-inhibitory rebound spikes. As the autaptic coupling strength is weak, the inhibitory autaptic current can not induce the PIR spikes. With increasing the coupling strength, the inhibitory autaptic current can induce the PIR spikes and regulate the neuronal firing. The firing spike time of the neuron becomes accurate. Further increasing the coupling strength, the effect of the PIR spikes is enhanced and the firing of the inhibitory autaptic neuron is also enhanced. With increasing the time delay, the time and shape of the inhibitory autaptic signal received by the neuron are changed and the effect of PIR also changes. That is why the accuracy of neuronal firing is changing with the time delay.

In the current work, we discuss this topic in a single neuron with autapse. The results reveal that both excitatory and inhibitory autaptic current could regulate the spike-timing precision. These results are also consistent with the experimental results.[25,26] The precise is believed to be a key factor in sensory information encoding.[1,2] On the one hand, the spike timing precision of the neurons play an important role in the synchronization of the neuronal circuits that generate persistent rhythms in the brain.[46] On the other hand, spike-timing precision is also crucial for establishing network oscillatory function and efficiency in cortical neurons.[45,46] It is also reported that the feedback synaptic current could stabilizes propagation of synchronous spiking and improve the spike-timing precision in cortical neural networks.[47] Here, we reveal that both of the excitatory and inhibitory autaptic current could impact on the spike-timing precision. Moreover, a precise spike pattern is used to transform information in cognitive and psychological processes in the nervous system.[3–5] Thus, it should be very interesting and valuable to expand the current research to the network level and discuss the behavior of spike-timing precision of spikes on the network in future work.

Acknowledgements

Project supported by the Fundamental Research Funds for the Central Universities, China (Grant No. GK201903020), the National Natural Science Foundation of China (Grant No. 12005006), and Scientific research project of Education Department of Gansu Province, China (Grant No. 2016A-049).

References

[1] Gardner B and Grüning A 2016 *PloS One* **11** e0161335
[2] Gaudry Q, Hong E J, Kain J, de Bivort B L, Wilson R I, de Bivort B L and Wilson R I 2013 *Nature* **493** 424
[3] Buzsáki G and Wang X J 2012 *Annu. Rev. Neurosci.* **35** 203
[4] James L E, Jean-Christophe L M, Glenn F, Zachary W and Monica Z W 2000 *Proc. SPIE* **4126** 407519
[5] Mainen Z and Sejnowski T 1995 *Science* **268** 1503
[6] Dayan P and Abbott L F 2001 *Theoretical Neuroscience* (Cambridge: The MIT Press)
[7] Butts D, Weng C, Jin J, Yeh C, Lesica1 N, Alonso J and Stanley G 2007 *Nature* **449** 92
[8] Buracas G T, Zador A M, DeWeese M R and Albright T D 1998 *Neuron* **20** 959
[9] Masuda N and Aihara K 2003 *Neural Comput.* **15** 1341
[10] Tzounopoulos T and Kraus N 2009 *Neuron* **62** 463
[11] VanRullen R, Guyonneau R and Thorpe S J 2005 *Trends Neurosci.* **28** 1
[12] Grothe B and Klump G M 2000 *Curr. Opin. Neurobiol.* **10** 467
[13] Borst A and Theunissen F E 1999 *Nat. Neurosci.* **2** 14731
[14] Fricker D and Miles R 2001 *Neuron* **32** 771
[15] Kilinc D and Demir A 2018 *J. Comput. Neurosci.* **44** 341
[16] Srivastava K H, Holmes C M, Vellema M, Pack A R, Elemans C P, Nemenman I and Sober S J 2017 *Proc. Natl. Acad. Sci. USA* **114** 1171
[17] Hasse J M and Briggs F 2017 *Proc. Natl. Acad. Sci. USA* **114** E6222
[18] Yao Y, Su C and Xiong J 2019 *Physica A* **531** 121734
[19] Verschueren E, Vanthornhout J and Francart T 2020 *Hear. Res.* **403** 108175
[20] Vogels T P, Froemke R C, Doyon N, Gilson M, Haas J S, Liu R, Maffei A, Miller P, Wierenga C J and Woodin M A 2013 *Front. Neural Circuits* **7** 119
[21] Garrido J A, Eduardo R and Egidio D 2013 *Front. Comput. Neurosc.* **7** 159
[22] Maisel B and Lindenberg K 2017 *Phys. Rev. E* **95** 022414
[23] Park S and Kwag J 2012 *Neurosci. Lett.* **523** 9
[24] Zhao Z, Li L and Gu H 2018 *Front. Cell. Neurosci.* **12** 00062
[25] Bacci A, Huguenard J R and Prince D A 2003 *J. Neurosci.* **23** 859
[26] Klausberger T, Magill P J, Marton L F, Roberts J D, Cobden P M, Buzsaki G and Somogyi P 2003 *Nature* **421** 844
[27] Hájos N, Pacutealhalmi J, Mann E O, Nacuteemeth B, Paulsen O and Freund T F 2004 *J. Neurosci.* **24** 9127
[28] Somogyi P and Klausberger T 2005 *J. Physiol.* **562** 9
[29] Bacci A and Huguenard J R 2006 *Neuron* **119** 2006
[30] Wang H and Chen Y 2015 *Chin. Phys. B* **24** 128709
[31] He Z, Yao C, Shuai J and Nakano T 2020 *Chin. Phys. B* **29** 128702
[32] Yue Y, Liu L, Liu Y, Chen Y, Chen Y and Yu L 2017 *Nonlinear Dyn.* **90** 2893
[33] Zhang N, Li D and Xing Y 2021 *Eur. Phys. J. B* **94** 1
[34] He Z, Yao C, Shuai J and Nakano T 2020 *Chin. Phys. B* **29** 128702
[35] Chagnaud B P, Perelmuter J T, Forlano P M and Bass A H 2021 *Elife* **10** e59390
[36] Xu Y and Ma J 2021 *Chin. Phys. B* **30** 100501
[37] Dhamala M, Jirsa V K and Ding M 2004 *Phys. Rev. Lett.* **92** 074104
[38] Wang Z, Parastesh F, Rajagopal K, Hamarash I I and Hussain I 2020 *Chaos Solitons Fractals* **134** 109702
[39] Khan M A, Maity D and Jabeen S D 2019 *Int. J. Mod. Phys. B* **33** 1950213
[40] Hodgkin A L and Huxley A F 1952 *J. Physiol.* **117** 500
[41] Chen Y, Zhang H, Wang H T, Yu L and Chen Y 2013 *PLoS One* **8** e56822
[42] Ding X, Jia B, Li Y and Gu H 2021 *Int. J. Mod. Phys. B* **35** 2150110
[43] Beiderbeck B, Myoga M H, Müller N I C, Callan A R, Friauf E, Grothe B and Pecka M 2018 *Nat. Commun.* **9** 1771
[44] Kilinc D and Demir A 2018 *J Comput Neurosci* **44** 341
[45] Gregory L P, Richard B L, Amanda M F and Ralph F F 2015 *J. Neurophysiol.* **113** 1862
[46] Sejnowski T J and Paulsen D 2006 *J. Neurosci.* **26** 1673
[47] Moldakarimov S, Bazhenov M and Sejnowski T J 2015 *Proc. Natl. Acad. Sci. USA* **112** 2545